RGNZ/MGPB

Quantitative Risk Assessment of the Effect of Sand on Multiphase Flow in a Pipeline

Rudarsko-geološko-naftni zbornik
(The Mining-Geology-Petroleum Engineering Bulletin)
UDC: 622.3:553.9
DOI: 10.17794/rgn.2022.4.4

Original scientific paper

Ugochukwu I. Duru[1]*; Princewill M. Ikpeka[1,3]; Chiziterem Ndukwe-Nwoke[1]; A. O. Arinkoola[2]; Stanley I. Onwukwe[1]

[1] *Department of Petroleum Engineering, Federal University of Technology, Owerri, Nigeria*

[2] *Chemical Engineering Department, Ladoke Akintola University of Technology, Ogbomoso, Nigeria.*

[3] *School of Computing Engineering and Digital Technologies, Teesside University, Middlesbrough, United Kingdom, TS1 3BX, https://orcid.org/0000-0002-1174-1491*

Abstract

The presence of sand particles flowing along with reservoir fluids in a pipeline increases the probability of pipeline failure. The risk of pipeline failure is either accentuated or abated by the flow conditions of the fluids in the pipeline. In this study, a quantitative risk analysis of the effect of sand on pipelines during multiphase flow, under the pipeline failure modes; sanding up, erosion, and encountering abnormal pressure gradient was conducted. Three piping components were considered: line pipe (nominal size 1.5 in [3.8 cm]), swing check valve (nominal size 12.007 in [30.5cm]) and 90 deg LR Elbow (nominal size 2.25 in [5.7cm]). Correlations that indicate the critical velocities and the critical sand concentrations above/below which these failures occur were employed and implemented in a Visual Basic program. The analysis was conducted at a temperature of 204°C and pressure of 604 psi [4.2×10^6 Pa]. A probability distribution, simulating real-life scenarios was developed using Monte Carlo simulation. This determines the probability of deriving critical sand concentration values that fall beyond the set statistical limits which indicates the probability of occurrence of the failure being investigated. For all three failures, the severity of occurrence (represented by CAPEX incurred in solving the failures) was multiplied with the probability of failure which gave rise to the risk indexes. Based on the histogram plot of average risk index and analysis, the study reveals that larger diameter components are prone to turbulence which lead to a greater risk of erosion. The risk of abnormal pressure drop and sanding up were considerably lower than for erosion (abrasion).

Keywords:

average particle diameter; critical sand concentration; sanding up; erosion; abnormal pressure gradient; Monte Carlo simulation

1. Introduction

For oil to flow from the reservoir to the surface, the pressure at the sandface must be greater than that at the wellhead. The amount of solid fines produced alongside oil is proportional to the stress exerted on the formation and subsequent rock failure (**Ben Mahmud et al., 2020**). Some factors that contribute to rock failure include: movement of tectonic plates, depth of burial, pore pressure, and also producing fluid drag force (**Nwabueze et al., 2012**). Therefore, several sand control techniques have been adopted by oil producing companies, such as chemical consolidation, screens, slotted liners, special filters, gravel packing, propped fracturing, selective perforating and production rate control (**Tronvoll et al., 2001**). These sand control techniques are designed to reduce the concentration of solid particles produced along with the reservoir fluids to insignificant amounts. However, the gradual accumulation of these solid particles over time results in surface equipment erosion, loss of production due to the accumulation of solid particles and equipment downtime. As much as separators might handle impurities from produced crude oil, there have been cases of flow of solid particles from the subsurface. As a result of this, sand flowing along with formation fluids causes flowline/pipeline failure downstream, consequently requiring the flowlines to be replaced or rehabilitated when they fail. It becomes very necessary to know what flow condition(s) poses the greatest risk, so as to optimize flow assurance and minimize pipeline/flowline failure. Pipeline/component failure can be determined by the prevalent flowing velocities for any combination of flow conditions (phase, regime, viscosity, particle densities, average diameters, and concentrations). Researchers have earlier conducted experimental investigations to observe particle behaviour and developed relevant correlations to predict the deposit velocity

Corresponding author: Ugochukwu I. Duru
e-mail address: ugochukwu.duru@futo.edu.ng

in hydraulic slurry transport pipeline (**Fitton, 2015; Bello and Oyeneyin, 2016; Bbosa et al. 2017**). These correlations were developed based on different settling velocity definitions and classified into six main definitions: sliding bed velocity, saltation velocity, suspending velocity, limiting deposit velocity, critical velocity, and the homogenous flow velocity. The critical velocity (the velocity corresponding to a minimum in the pressure gradient versus velocity curve) does not require observations of the flow regime and is usually assumed to be higher than the suspending velocity and it is used for safe design. Considering this, analyses on sand effects were conducted with reference to critical velocity. In situations where critical velocity, V_c could not be explicitly derived, the Minimum Transport Condition (MTC) was calculated for safe designs. **Thomas (1961)** defined MTC, as the minimum velocity demarcating flows in which the sand forms a bed at the bottom of the pipe from fully suspended flows. This study is purely a modeling approach to generate critical sand concentration (CSC) data for all failure modes in Visual Basic for Excel using adopted and adapted correlations as VBA code.

2. Methodology

A number of models were adopted and adapted for use in Visual Basic as defined in the next sub-section to generate CSC. For each model used, sensitivities to the laminar or turbulent flow regime and given flow parameters were analyzed. Monte Carlo simulation was used to generate probability distributions that closely simulate real-life scenarios given the constraints of flow parameters available. Three piping components were considered for failure analysis: Line pipe, swing check valve and 90-deg LR elbow (see **Figure 1**). Five nominal sizes of each component were analyzed. The input data employed in this study and their sources are given in **Tables A** and **B** (Appendix A).

Forty-five failure modes were considered: three failure types for three piping components for five different sets of diameters. To evaluate the three failure modes, key multiphase flow **Equations 1-9** were extracted from literature and applied in this model.

i. Critical Sand Velocity, V_c: determined using **Salama (2000)** modified model.

$$V_c = \left[(V_{SL})^{0.5} \times d_p^{0.17} \times \left(\frac{\mu_l}{\rho_l} \right)^{-0.09} \times \left(\frac{\rho_p - \rho_l}{\rho_l} \right)^{0.55} \times D^{0.47} \right]^{\frac{1}{1.73}} \quad (1)$$

Where:

V_c – critical sandup velocity [m/s],
V_{SL} – superficial liquid velocity [m/s],
d_p – average particle diameter [m],
μ_l – multiphase liquid viscosity [m²/s],
ρ_l – multiphase liquid density [kg/m³],
ρ_p – particle density [kg/m³],
D – piping component internal diameter [m].

ii. Particle Settling Velocity (Laminar), u_t; for laminar flow, Stoke's law was used

$$u_t = \frac{g \times d_p^2 \times (\rho_p - \rho_l)}{18 \times \mu_l} \quad (2)$$

iii. Particle Terminal Settling Velocity (Turbulent), u_t; determined according to Newton's Law for Turbulent Settling

$$u_t = 1.73 \sqrt{d_p \times g \times \left(\frac{\rho_p - \rho_l}{\rho_l} \right)} \quad (3)$$

Where:

u_t - terminal settling velocity [m/s],
g *or* g_c - acceleration due to gravity [m/s²].

iv. Friction Velocity (Laminar), u_0^*; **Thomas (1961)** Upper Model was used

$$u_0^* = \left[100 \times u_t \times \left(\frac{v_l}{d_p} \right)^{2.71} \right]^{0.269} \quad (4)$$

Where:

u_0^* – friction velocity, ft/sec [m/s],
v_l – liquid velocity without considering holdup, ft/sec [m/s].

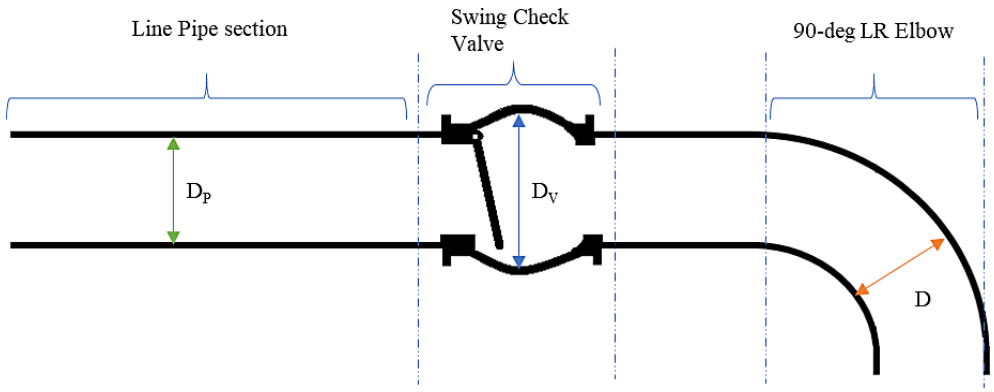

Figure 1: Piping components considered for failure analysis

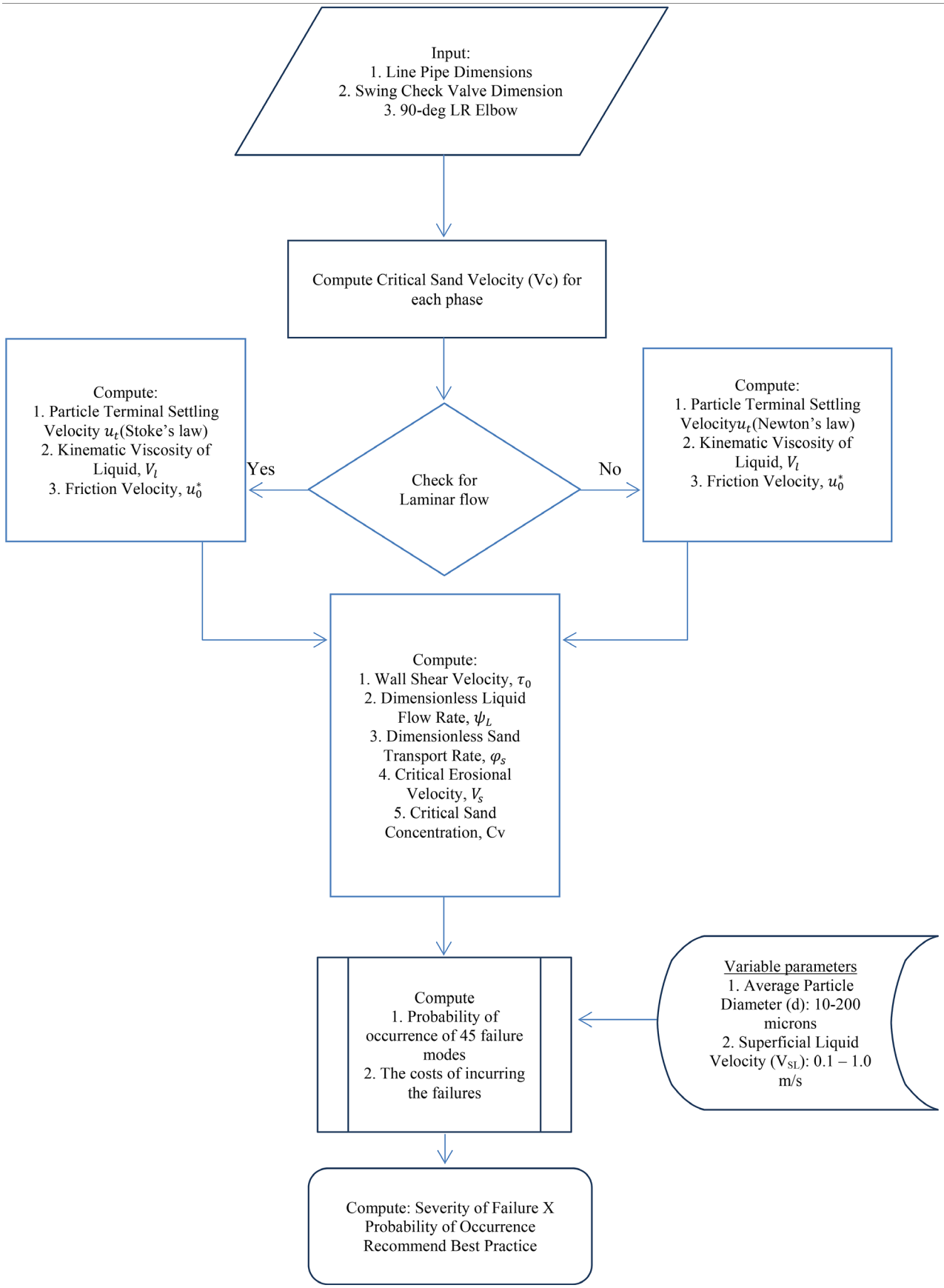

Figure 2: Flowchart of Computation Process

v. Friction Velocity (Turbulent), u_0^*; **Thomas (1961)** Lower Model was applied

$$u_0^* = \left[0.204 u_t \times \left(\frac{v_l}{d_p} \right) \times \left(\frac{v_l}{D} \right)^{-0.6} \times \left(\frac{\rho_p - \rho_l}{\rho_l} \right)^{-0.23} \right]^{0.714} \quad (5)$$

vi. Dimensionless Liquid Flow (ψ_L) *and Sand Transport Rate* (φ_s); the **Gillies (1997)** model was used

$$\psi_L = \frac{\rho_l \times g \times d_p \times \left(\frac{\rho_p}{\rho_l} - 1 \right)}{\tau_0} \quad (6)$$

$$\varphi_s = \left[\frac{4}{\psi_L} - 0.188 \right]^{1.5} \quad (7)$$

Where:

ψ_l – Gillies (1997)'s dimensionless liquid flow rate,

φ_s – Gillies (1997)'s dimensionless sand transport rate,

ρ_m – multiphase mixture (liquid and gas) density [kg/m^3].

vii. Pressure Drop at MTC; this was based on **King et al (2000)** model

$$\left| \frac{\Delta P}{\Delta x} \right|_{MTC} = \frac{4 \times \rho_l \times \left(u_0^* \right)^2}{g_c \times D} \quad (8)$$

Where:

$\left| \frac{\Delta P}{\Delta x} \right|_{MTC}$ – pressure drop at minimum transport condition [Pa].

viii. Critical Sand Concentration: **Kokpinar and Gogus (2000)** model was used

$$C_v = \left(\frac{V_c}{\sqrt{gD} \times 0.055 \left(\frac{d_p}{D} \right)^{-0.6} (s-1)^{0.07} \left(\frac{\rho_l u_t d_p}{\mu_l} \right)^{0.3}} \right)^{\frac{1}{0.27}} \quad (9)$$

Where:

C_v – critical sand concentration [ppm],

V_p – critical velocity associated with the pressure drop at MTC [m/s].

The probabilities of occurrence of the individual 45 failure modes for each "n" operating condition were obtained. The "n" operating conditions refer to the changing input variables in the calculations done with the VBA software, which are the eleven discretized superficial liquid velocity values from 0 to 1 ms^{-1}. This is for twenty different average particle diameters, giving n = 220 different operating scenarios (in cases where turbulence occurred and for erosional analysis). The flowchart of the computation process is as shown in **Figure 2.**

The costs of incurring the failures considered in this study include:

1. Cleaning up sanded up API 5L line pipes through epoxy flood coating, for all 5 dimensions as against continuous operation;
2. Cleaning up sanded up ASME B16.9 Class 1500 swing check valves through epoxy flood coating, for all 5 dimensions as against continuous operation;
3. Cleaning up sanded up ASME B16.10 90-degrees long radius elbows through epoxy flood coating, for all 5 dimensions as against continuous operation;
4. Replacing eroded API 5L Line Pipes, for all 5 dimensions as against continuous operation;
5. Replacing eroded ASME B16.9 Class 1500 swing check valves, for all 5 dimensions as against continuous operation;
6. Replacing eroded ASME B16.10 90-degrees long radius elbows, for all 5 dimensions as against continuous operation;
7. Restoring normal pressure gradient in API 5L line pipes through in-situ recoating, for all 5 dimensions as against continuous operation;
8. Restoring normal pressure gradient in ASME B16.9 Class 1500 swing check valves through in-situ recoating, for all 5 dimensions as against continuous operation;
9. Restoring normal pressure gradient in ASME B16.10 90-degrees long radius elbows through in-situ recoating, for all 5 dimensions as against continuous operation.

These costs served as severity rankings for risk analysis. A severity of failure against probability of occurrence operation was conducted to assess the risks involved in operating any of the piping components for all five internal diameter sets (45 case scenarios). Best practices were recommended based on the results.

The following assumptions or constraints were considered in this study:

1. Gas-Oil two-phase flow
2. Unknown original volume of sand introduced into the gas-oil flow
3. Horizontal pipe and isentropic flow
4. Uniform pipe diameter
5. Negligible effect of impact angle of sand on pipe walls
6. Steady-State flow
7. Original Water-Oil Ratio (WOR) is known.

3. Results and Discussions

The effect of sands in a multiphase flow were analysed and the results of the analysis were discussed under three failure modes: sanding-up, erosion and abnormal pressure drop. For each failure mode discussed, the sensitivity of the indicative parameter is measured with superficial liq-

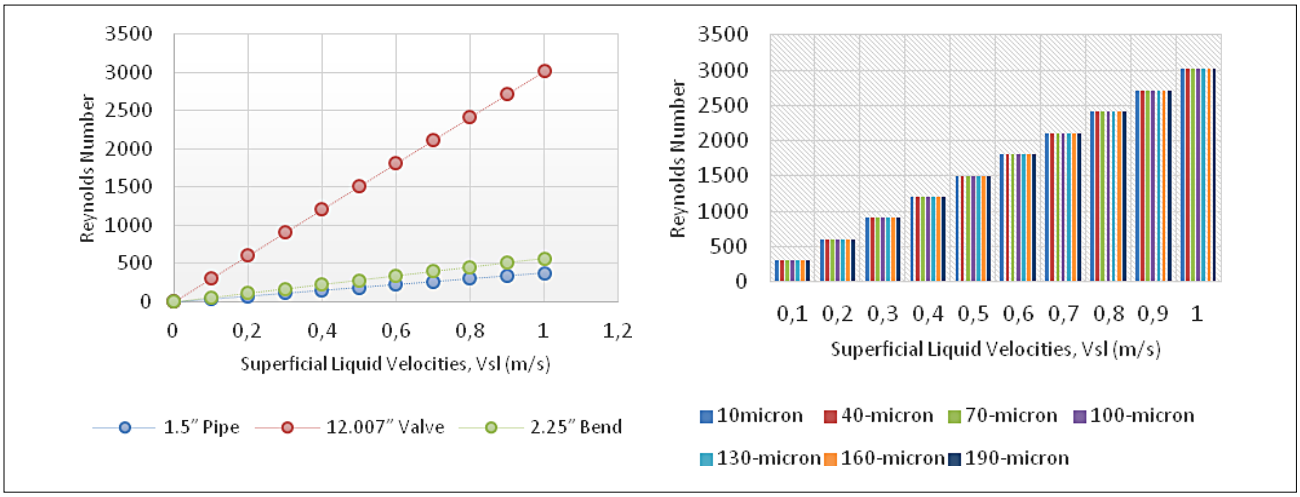

Figure 3: (a) Reynolds number vs superficial liquid velocities of 3 components **(b)** Reynolds number vs superficial liquid velocities for 12.007" valve at various particle diameter

Table 1: Superficial Liquid Velocity Points Where Turbulence Occurs

Valve Diameter (in.)	V_{sl} values for Turbulent Flow (m/s)
12.007	0.7 to 1
16.496	0.6 to 1
18.504	0.5 to 1
21.496	0.5 to 1
26.496	0.4 to 1

uid velocity. The sensitivity analysis allows us to capture the effect of flow velocity on each failure mode.

3.1 Failure Mode I: Sanding up

The failure mode for sanding-up, describes the degree to which each piping component is susceptible to sand build-up during normal operating conditions. To explore this failure mode, it would be necessary to understand the flow condition at each piping components. From the Reynolds number chart (see **Figure 3**), given the flow conditions under consideration (V_{sl}: 0 to 1 ms^{-1}; dp: 10 to 200 microns), only the valve components experienced turbulent flow, but not for all flow rates. Turbulent flow was considered for flows with N_{Re} >2000 (according to Newton's Particle Settling Law for Re_p >1000). Exploring further, the effect of particle size on the flow condition of the valve, it was observed that values of average particle diameter (dp) were not instrumental in determining turbulence of flow as expected.

From results, it can be observed that turbulent flow across the valves occurs under the conditions given in **Table 1**:

Due to the discrete nature of the variable inputs (even though it approximates a continuous distribution), the exact V_{sl} values where turbulence begins cannot be determined, unless this test can be conducted either experimentally or with a less discrete distribution. Critical sand velocity values were calculated for each piping component and the value obtained was used to quantify the sanding up risk at each piping component. From the analysis, it was observed that the swing check valve and line pipe components had the highest and lowest critical sand velocities respectively (see **Figure 4a**). The component with the least critical sand velocity (in this case 1.5 in line pipe) poses the greatest risk of sanding up during normal operations. This is reflected in the critical sand concentration (see **Figure 4b**).

3.1.1 Sensitivity of Critical Sand-up Velocity to Superficial Liquid Velocity (V_{sl}) and Particle Size Diameter

For this study, gas and oil is assumed to flow simultaneously through the piping components. The sand component is confined to the liquid phase and as such the critical sand velocity is affected by the superficial liquid velocity. A sensitivity analysis on the effect of superficial liquid velocity on critical sand velocity reveals a positive relationship: an increasing V_{sl} leads to a corresponding increase in critical sand-up velocity, V_c (see **Figure 5**). Similarly, the particle size diameter exhibits the same effect on the critical sand velocity. It could be observed that the critical velocity values for line pipe and elbow components were much closer compared to that of the valve. From this analysis it was deduced, that prevailing flow regime in each component is responsible for the disparity in critical sand-up velocity values.

3.1.2 Sensitivity of Critical Sand Concentration to Superficial Liquid Velocity (V_{sl}) and Particle Size Diameter

Conducting a sensitivity analysis on critical sand concentration, it was observed that while the superficial liquid velocity exhibits a positive relationship with sand

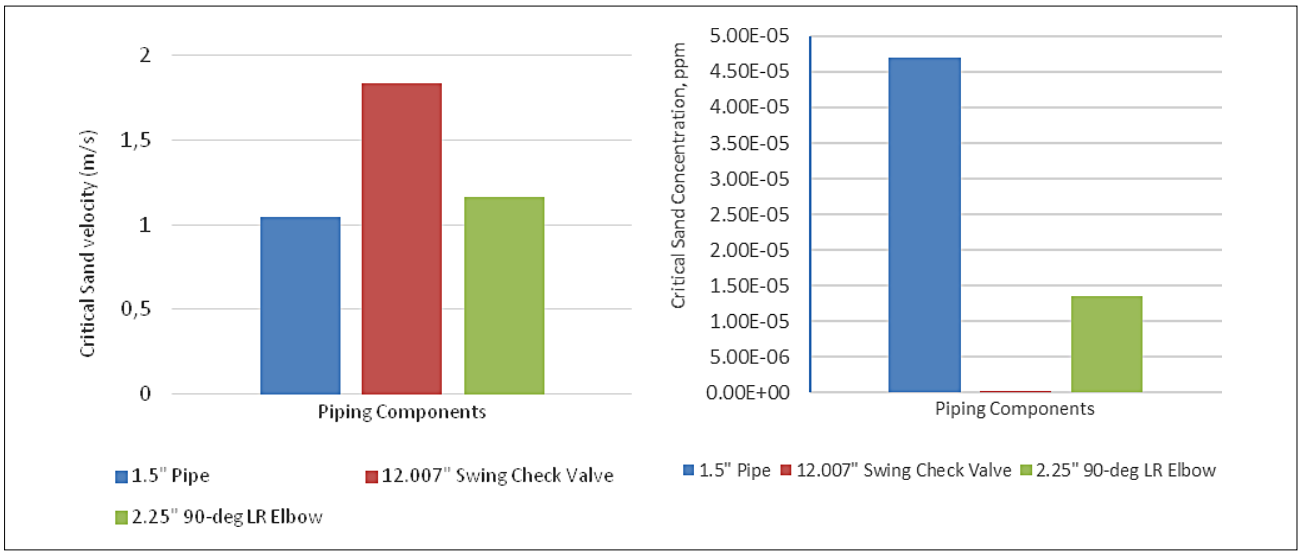

Figure 4: **(a)** Critical sand-up velocity **(b)** Critical sand concentration for each piping component

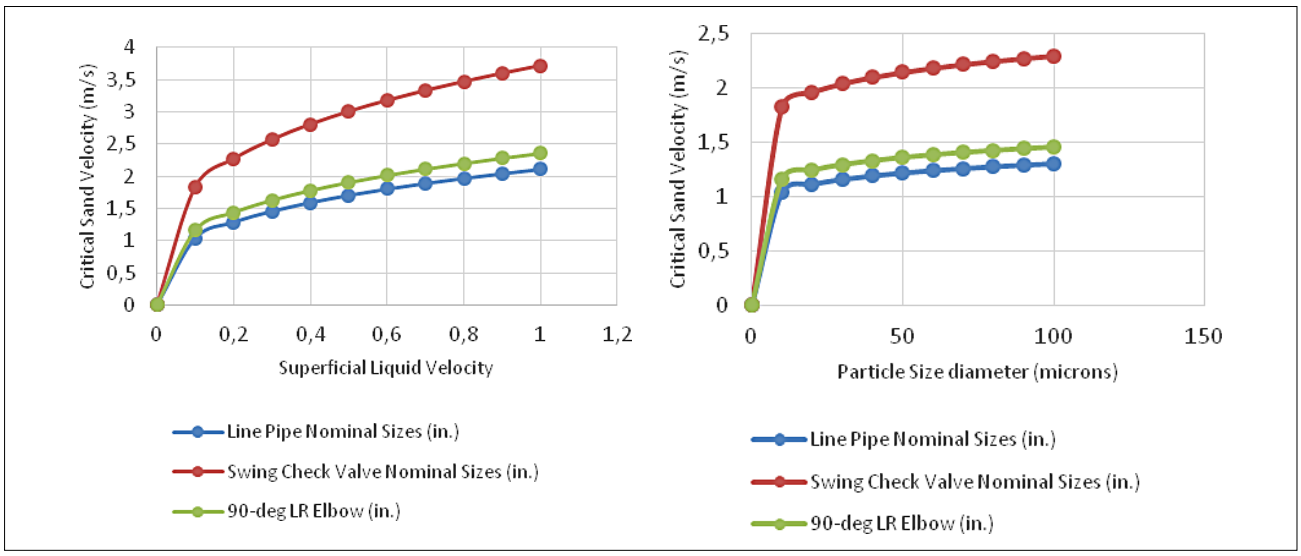

Figure 5: Sensitivity analysis of critical sand velocity to **(a)** superficial liquid velocity **(b)** particle size diameter

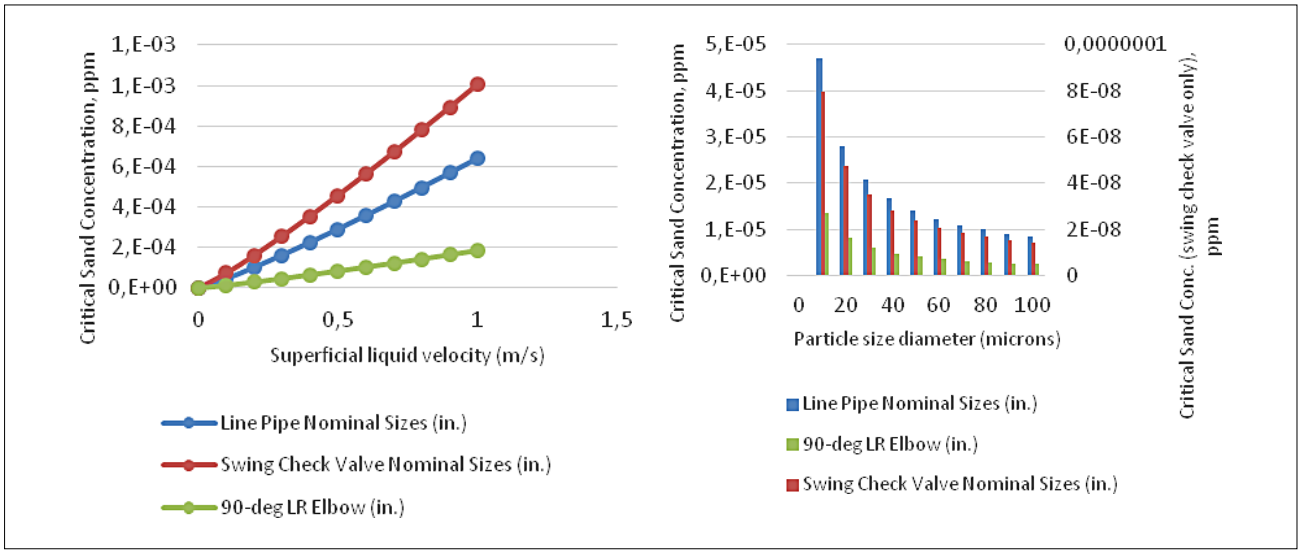

Figure 6: Sensitivity analysis of critical sand concentration to (a) superficial liquid velocity (b) particle size diameter

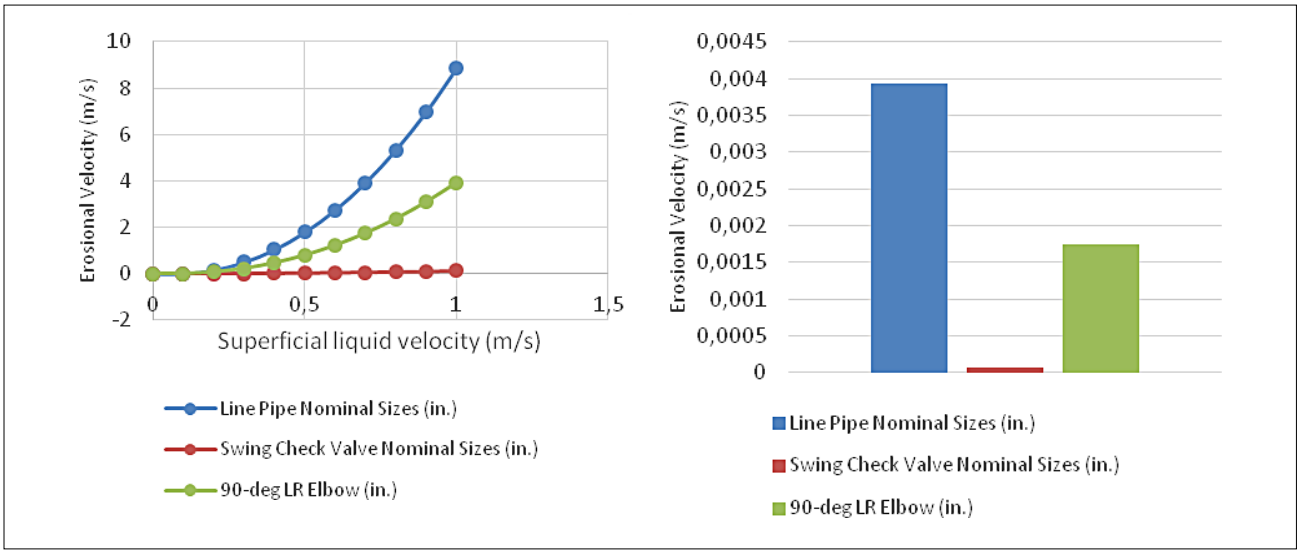

Figure 7: (a) Erosional velocity of each pipe component during normal operating condition. (b) Sensitivity of erosional velocity to superficial liquid velocity

concentration, the particle size diameter showed a negative relationship (as observed in **Figure 6**).

3.2 Failure Mode II: Erosion

To quantify this failure mode, the erosion velocity was calculated for each piping component. Erosional velocity describes the velocity above which particle erosion due to abrasion occurs. Considering this, pipe components with higher erosional velocity have a lower probability of failure during normal operating conditions. The erosional velocity (V_s) values obtained revealed that the swing check valve is the most susceptible component to erosion (see **Figure 7a**). Performing a sensitivity analysis of the erosional velocity to superficial liquid velocity, a positive relationship was observed on all three piping components (see **Figure 7b**).

From the obtained results, at superficial liquid velocity of 1 m/s, the erosional velocity which should not be superseded to avoid abrasion of line pipe components, is 8.9 m/s for average particle diameters of 10 microns and

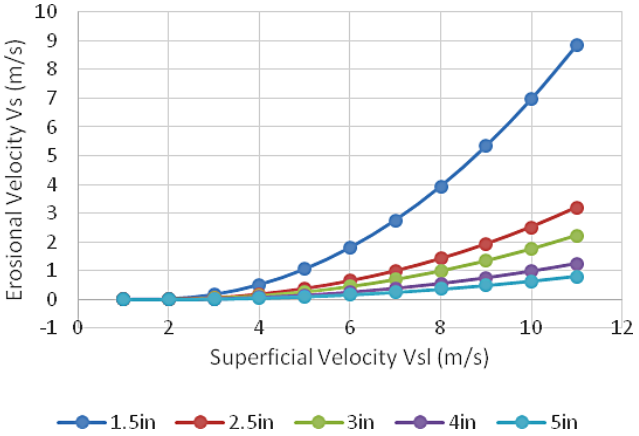

Figure 8: Critical erosional velocity chart depicting effect of internal diameter

4 m/s for 90 deg elbow component. The reason for this was that, given flow conditions and from known experimental results (**Arabnejad et al., 2013; Zhang et al., 2016**), particles with smaller diameters pose a threat to pipe integrity when it comes to abrasion. Also, the trend showed that, for the particle diameter values that do have V_s values, the V_s values are bigger for components with bigger internal diameters (IDs) (see **Figure 8**). This implies a higher likelihood for a component with bigger IDs to suffer from abrasion, because components with bigger IDs support turbulent flow the most for a particular set of flow conditions. These findings are consistent with results given by **Salama (2000)**.

3.3 Failure Mode III: Abnormal Pressure Drop

The trends for (Critical Velocity for Abnormal Pressure Drop) V_p values and the Pressure Drop at MTC values are similar to critical velocity V_c trends, except for the portion for valves that is affected by turbulence (see **Figure 9**).

Components with bigger ID exhibit higher pressure gradients, which when exceeded, cause abnormalities in flow (surges that can lead to ruptures, bursts, etc.). Finally, the CSC values showed a reverse trend with V_c, V_s, and V_p values. This is so because, while V_c represents a velocity which must be exceeded to prevent sanding up, CSC for V_c represents the maximum sand concentration that satisfies this condition set by V_c (the same goes for V_p). This is because; the bigger the concentration, the more likely sanding up and pressure surges can occur. Also, while V_s represents a velocity which must not be exceeded to prevent abrasion, CSC for V_s represents the minimum sand concentration to satisfy set condition by V_s, since the smaller the concentration, the more harmful the particle to the pipe.

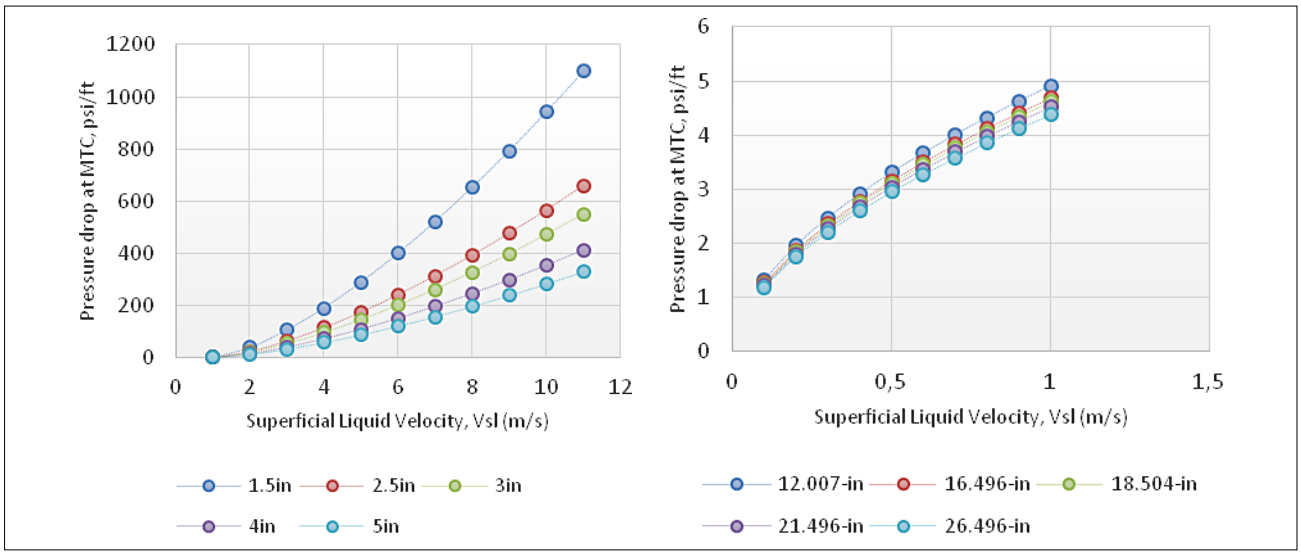

Figure 9: Critical pressure drop at MTC Chart for (a) Line pipe 1.5-5in ID (b) Valve 12.007- 26.496in ID

4. Probability Distribution of Failure Occurrence

DiscoverSim®'s Monte Carlo probability simulations were run on all 45 scenarios. The input parameters were particle diameter dp, superficial liquid velocity V_{sl}, and component diameter. While the output parameters investigated were critical velocity, erosional velocity, velocity at MTC pressure drop and critical sand concentration. 10,000 scenarios were run using established statistical

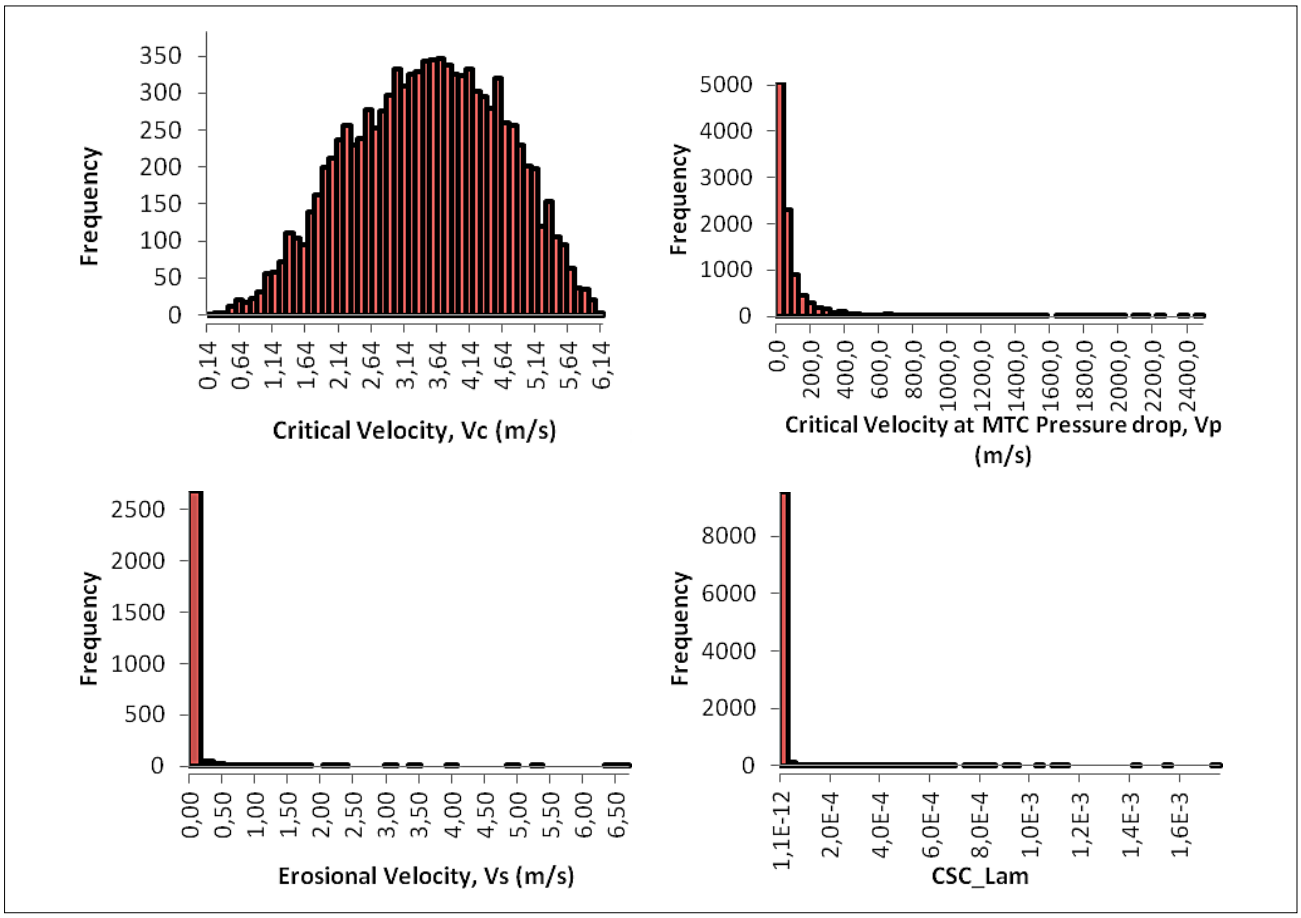

Figure 10: Frequency distribution chart generated for all 45 scenarios for (a) critical velocity (b) critical velocity at MTC pressure drop (c) erosional velocity (d) critical sand concentration

Table 2: Key results for simulation run in Figure 10

Descriptive Statistics	Critical Velocity, Vc (m/s)	Critical Velocity at MTC Pressure drop, Vp (m/s)	Erosional Velocity, Vs (m/s)	Critical Sand Concentration, CSC
Count	10000.000	10000.000	2786.000	10000.000
Mean	3.498	103.020	0.042	0.000
Standard Deviation	1.141	200.471	0.294	0.000
Range	6.031	2494.139	6.699	0.002
Minimum	0.142	0.001	0.000	0.000
25th Percentile (Q1)	2.647	16.233	0.000	0.000
50th Percentile (Median)	3.539	44.755	0.001	0.000
75th Percentile (Q3)	4.374	96.536	0.007	0.000
Maximum	6.174	2494.140	6.699	0.002

tools that simulate real life scenarios, and the probability distributions were generated. The results are shown in **Figure 10**.

Table 3: Tolerance values used to determine ideal conditions

Failure Mode	Tolerance
Sanding Up	+7%
Erosion	-3%
Abnormal Pressure Drop	+5%

Table 4: QRA for Sanding Up

Quantitative Risk Assessment (Sanding Up) By Sets					
Sets	Component				
	QR for Pipe	QR for Valve	QR for Bend	Total Risk	Average Risk
Set 1	11.50	0.00	1.23	12.73	4.24
Set 2	1.19	0.00	2.09	3.28	1.09
Set 3	1.53	0.00	2.50	4.03	1.34
Set 4	0.00	0.00	0.00	0.00	0.00
Set 5	0.00	0.00	3.79	3.79	1.26
Total Risk = QR(pipe)+QR(valve)+QR(bend)					
Average Risk = Total Risk / 3					

Table 5: QRA for Erosion

Quantitative Risk Assessment (Erosion) By Sets					
Sets	Component				
	QR for Pipe	QR for Valve	QR for Bend	Total Risk	Average Risk
Set 1	829.98	7.91	11.77	849.66	283.22
Set 2	835.40	6.01	12.10	853.50	284.50
Set 3	827.82	5.00	11.82	844.64	281.55
Set 4	857.20	5.00	12.47	874.67	291.56
Set 5	834.99	4.00	11.59	850.58	283.53
Total Risk = QR (pipe)+QR(valve)+QR(bend)					
Average Risk = Total Risk / 3					

The relevant information extracted from the statistical analysis were the probability distribution shape and statistical parameters captured in **Table 2**. To generate the plot discrete in **Figure 10**, it is important to note that particle diameter and line pipe component diameters were modelled as uniform discrete variables with an equal probability of occurrence. The superficial velocity on the other hand was modelled as a uniform continuous variable.

The probability distribution shape is influenced by a lot of factors, but for this study's considerations, it is worthy to note that only the critical velocity showed a particular PERT distribution. The CSC values are highly skewed towards the lowest Ideal CSC value. Ideal CSC value = tolerance*Actual CSC value. Actual CSC value is equal to the average CSC value for each of the 45 case scenarios. The tolerance values were determined considering the possibility of errors and are given in **Table 3**. The reason for this high skewing is because the statistical limits (determined by multiplying the tolerance percentages with the highest CSC value in each 45 distribution for failure through sanding up and abnormal pressure drop, or the tolerance percentages with the lowest CSC value in each 45 distribution for failure by erosion), upper sanding limit (USL) or lower sanding limit (LSL),

Table 6: QRA for Abnormal Pressure Drop

Quantitative Risk Assessment (Abnormal Pressure Drop) By Sets					
Sets	Component				
	QR for Pipe	QR for Valve	QR for Bend	Total Risk	Average Risk
Set 1	31.05	0.13	0.45	31.63	10.54
Set 2	31.70	0.00	0.47	32.17	10.72
Set 3	32.16	0.01	0.48	32.65	10.88
Set 4	33.04	0.00	0.06	33.10	11.03
Set 5	33.93	0.00	0.52	34.45	11.48
Total Risk = QR(pipe)+QR(valve)+QR(bend)					
Average Risk = Total Risk / 3					

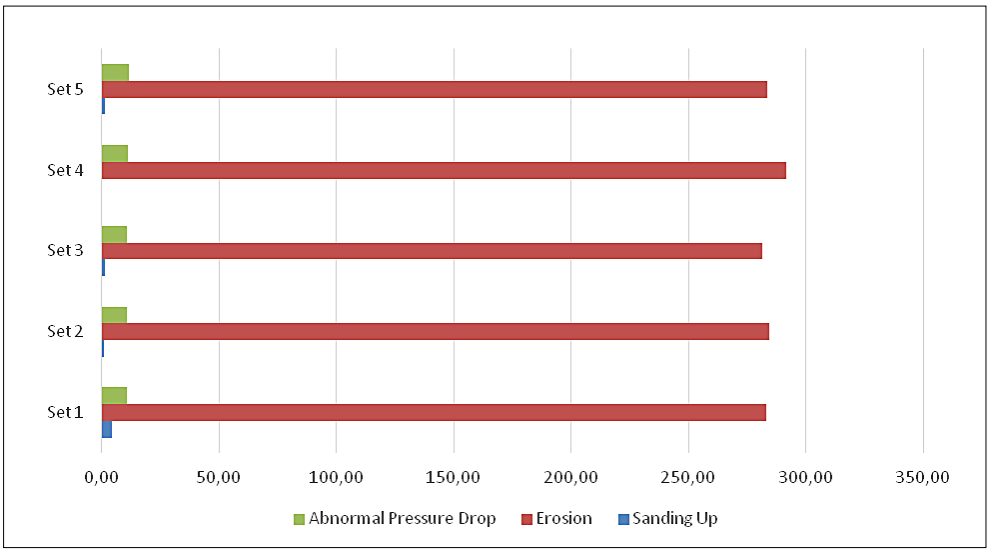

Figure 11: Histogram Plot of all three QRAs, for all five sets (NOTE: Phase = set)

and the ideal CSC values create a highly wide ranged probability distribution, with a majority of the outcomes within the perimeter of the ideal CSC value, and a few stray outcomes very far from it. The Spearman Rank correlation was used to determine which of the input distribution was most responsible for causing the eventual probability output. It can be observed that all the time, it was the velocity values that most influence the eventual CSC probability output, as it should be. In a few cases though (abnormal pressure drops for set 1, and the 2.25" bend distribution for erosional failure), the average particle diameter actually had a large role to play in determining distribution. For the abnormal pressure drop, this is to be expected since by common sense, the larger the particle size, the more effective it should be at causing failures in pressure drop.

The out-of-spec and within-spec values determine the percentage of outcomes that either fall out of statistical limits set (USL or LSL), or stay within the statistical limit, respectively. The out-of-spec values are quite interesting, as they form the ranking (in %) used to evaluate the probability of the occurrence of these failures being studied and are employed in the quantitative risk analysis done on these failure modes for the 5 sets. Quantitative risk assessment was performed by multiplying the probability of occurrence (MC's out-of-spec values) with severity of failure. **Tables 4 to 6** and histogram plot (see **Figure 11**) summarize the risk values obtained and how they were analyzed.

It can be seen from the plot that the risk of encountering erosion is highest for all 5 sets, followed by the risk for encountering abnormal pressure gradient. The sanding up risk is infinitesimal compared to others and in a case where all conditions necessary for all failure modes to occur are evident, it would be within reason to handle erosion (replace piping component), abnormal pressure gradient (in-situ recoating), and sanding up (epoxy flood coating), in order of priority. This work did not consider a base-case scenario (a case study). **Figure 11** is instrumental when compared with a given case study operating with flow conditions similar to the ones used in this paper. This enables one to evaluate the risk to continue flow through a pipe or to consider the solutions to pipeline failure as presented in this paper.

5. Conclusion

Of the three piping components considered, the results obtained from this study reveal that turbulence occurred only across the valve component. Higher values of internal diameter of each component, resulted in a corresponding increase in Reynolds number. This agrees with experimental works by (**Abd et al., 2019; Nur et al., 2019**). In addition to this, it was also observed that turbulence did not affect the ability of particles to sand up under the given flow conditions. This means that if particles do sand up during turbulent flow, it was not as a result of the turbulence, but of other velocity-related factors. Given flow conditions, erosion through abrasion of pipe inner walls was not observed when average particle diameter greater than 20 microns were analyzed. Also, the ability to erode increases with an increase in internal diameter due to turbulence. Other conclusions that can be drawn from this study include:

- The size of average particle diameter plays a significant role in determining critical sand concentration that could cause abnormal pressure-drop, unlike erosion and sanding up failures;
- The critical velocity value is the major factor that determines the critical sand concentration;
- The hierarchy of engendering risk for each failure mode is giving as: erosion → abnormal pressure drop → sanding up;
- The best practice, if economically feasible, must completely replace the affected piping component.

It is recommended that further experimental work should be conducted on this study with a base case to compare with the simulated cases.

Acknowledgement

The authors express their gratitude to the Technical Staff at the Department of Petroleum Engineering Computer Lab., Federal University of Technology, Owerri, Nigeria for always getting the laboratory ready for use.

6. References

Abd, H. M., Alomar, O. R., and Mohamed, I. A. (2019): Effects of varying orifice diameter and Reynolds number on discharge coefficient and wall pressure. Flow Measurement and Instrumentation, 65, 219–226. https://doi.org/10.1016/j.flowmeasinst.2019.01.004

API. (2004): API Specification 5L. Specification for Line Pipe. American Petroleum Institute. API Publishing Services, Washington, D.C. www.api.org, 108-116

Arabnejad, H., Shirazi, S. A., McLaury, B. S., and Shadley, J. R. (2013): Calculation of erosional velocity due to liquid droplets with application to oil and gas industry production. Proceedings - SPE Annual Technical Conference and Exhibition, 5, 4030–4042. https://doi.org/10.2118/166423-ms

ASME. (2007): ASME B16.9: Factory-Made Wrought Buttwelding Fittings. American Society of Mechanical Engineers, www.asme.org, 44

Bbosa, B., DelleCase, E., Volk, M. and Ozbayoglu, E. (2017): A Comprehensive Deposition Velocity Model for Slurry Transport in Horrizontal Pipelines. J Petrol Explor Prod Technol 7, 303-310. https://doi.org/10.1007/s13202-016-0259-1

Bello, K. and Oyeneyin, B. (2016): Experimental Investigation of Sand Minimum Transport Velocity in Multiphase Fluid Flow in Pipes. Nigerian Journal of Technology (NIJOTECH) 35, 3, 531-536.

Ben Mahmud, H., Leong, V. H., and Lestariono, Y. (2020): Sand production: A smart control framework for risk mitigation. Petroleum, 6, 1, 1–13. https://doi.org/10.1016/j.petlm.2019.04.002

El-Alej, M. E. (2014): Monitoring Sand Particle Concentration in Multiphase Flow Using Acoustic Emission Technology. Cranfield University.

El-Alej, M., Mba, D., Yan, T., and Elforgani, M. (2013): Monitoring Sand Transport Characteristics in Multiphase Flow in Horizontal Pipelines Using Acoustic Emission Technology. International Journal of Mechanical Aerospace, Industrial, Mechatronic and Manufacturing Engineering, 7, 6, 1144-1150.

Fitton, T.G. (2015): A Deposit Velocity Equation for Open Channels and Pipees. Proceeding of 17th International Conference on transport and sedimentation of solid particles. September 22-25, 2015. Delft, The Netherlands.

Gillies, G. R., McKibben, M. J., and Shook, C. A. (1997): Pipeline Flow of Gas, Liquid and Sand Mixtures at Low Velocities. J.Ca.Pet.Tech, 36, 36-42.

King, M. J., P., F. C., and Hill, T. J. (2000): Solids Transport in Multiphase Flows Application to High Viscosity Systems. Energy Sources Tech Conference, New Orleans, 14-17.

Kokpinar, M. A., and Gogus, M. (2001): Critical Flow Velocity in Slurry Transporting Horizontal Pipelines. Journal of Hydraulic Engineering, 127, 763-771.

Nur, A., Afrianita, R., and Ramli, R. D. T. F. (2019): Effect of pipe diameter changes on the properties of fluid in closed channels using Osborne Reynold Apparatus. IOP Conference Series: Materials Science and Engineering, 602, 1. https://doi.org/10.1088/1757-899X/602/1/012058

Nwabueze, V. O., Onikoyi, A. S., Okoro, F. O., and Ajienka, J. A. (2012): Sanding in oil well reservoir completions. Society of Petroleum Engineers - 36th Nigeria Annual Int. Conf. and Exhibition 2012, NAICE 2012 - Future of Oil and Gas: Right Balance with the Environment and Sustainable Stakeholders' Participation, 1, 290–299. https://doi.org/10.2118/163010-ms

Tronvoll, J., Dusseault, M. B., Sanfilippo, F., Santarelli, F. J., Rock, O., Integrated, M., and Ormis, S. (2001): SPE 71673 The Tools of Sand Management.

Salama, M. M. (2001): Sand Production Management. Journal of Energy Resources Technology, 122, 29-33.

Thomas, D. G. (1962): Transport Characteristics of Suspensions Part VI. Minimum Transport Velcity of Large Particle Size Suspensions in Round Horizontal Pipes. AIChE J., 8, 3, 373-377

Appendix

Table A: Feed Data Set for Piping Component Dimensions (Source: API 5L Specs (2004) and ASME B16.9 (2012))

Sets	Line Pipe Nominal Sizes (in.)	Swing Check Valve Nominal Sizes (in.)	90-deg LR Elbow (in.)
1	1.5	12.007	2.25
2	2.5	16.496	3.75
3	3	18.504	4.5
4	4	21.496	6
5	5	26.496	7.5

Table B: Summary of Feed Data

Data	Value/Range	Unit	Remarks
Average Particle Diameter	10 – 200	microns	Derived from previous studies
Superficial Liquid Velocity	0 – 1	ms^{-1}	Derived from previous studies
Pipe Type	API 5L Seamless Pipe		Derived from API Specifications
Valve Type	ASME B16.10 Class 1500 Short-Pattern-Fixed Single Plate Wafer-Type Swing Check Valves		Derived from ASME Specifications
Bend Type	ASME B16.9 Specifications 90° Long Radius Elbow		Derived from ASME Specifications
Oil Type	90 RON Gasoline		RON = Research Octane Number; Typical Nigerian Gasoline
Gas Type	Natural Gas (HHV 54.3)		Typical Algerian Natural Gas
Particle Density:	2.65	g/cm^3	Derived from previous studies by Freeze and Cherry (1979)
Operating Temperature	204	°C	
Operating Initial Pressure (Also MAOP: Maximum Allowable Operating Pressure)	673	psi	25% of least MAWP (11.6 MPa or 1682.438 psi)
Oil Density:	57.78	lb/ft3	At 20 °C; Estimated from Typical Values
Oil API Gravity	70		Estimated from Typical Values
Oil Specific Gravity	0.702		Estimated from Typical Values
Oil Viscosity	0.97	cp	Estimated from Typical Values
Oil Vapour Pressure (Reid vapour pressure value)	11.603	psi	80 kPa; Estimated from Typical Values
Gas Viscosity	0.016	cp	Estimated from Typical Values
Gas Molecular Weight	18.147	Kg/kmol	Estimated from Typical Values
Gas Specific Gravity:	0.65		Estimated from Typical Values
Gas Density:	5.88	lb/ft3	Estimated from Typical Values
Gas Vapour pressure:	0.000015	Psi	0.101325 Pa (atmospheric); Estimated from Typical Values
Water Density:	24.37	lb/ft3	At 20 °C; Estimated from Typical Values
Water Specific Gravity:	1.07		Estimated from Typical Values
Water Viscosity:	0.16	cp	Estimated from Typical Values
Water-Oil Ratio (WOR):	0.01		Estimated from Typical Values
Liquid Holdup	0.507		Derived from previous studies
Gas Holdup/Void Fraction	0.493		Derived from previous studies
Oil Formation Volume Factor (Bo):	1.237	rb/stb	Estimated from Typical Values
Water Formation Volume Factor (Bw):	0.12	rb/stb	Estimated from Typical Values
Acceleration Due to Gravity:	32.2	ft/s^2	Estimated from Typical Values

Table C: Procedure of Usage of Visual Basic for Excel Coding

An Overview of VBA for Excel Codes Used to Determine Critical Sand up Velocities (Vc), Critical Erosional Velocities (Vs), Pressure Drop @ MTC and then its associated Critical Velocity Value (Vp), and the Critical Sand Concentrations (Cv).			
Value Being Determined	**Steps**	**Correlation**	**Sample VBA Code**
Vc	1: Critical Sand Velocity Determination	$V_c = \left[\left(V_{SL}\right)^{0.5} d_p^{0.17} \left(\frac{\mu_l}{\rho_l}\right)^{-0.09} \left(\frac{\rho_p - \rho_l}{\rho_l}\right)^{0.55} D^{0.47} \right]^{\frac{1}{1.73}}$ Modified Salama (2000) Model	Program Start Declare Variable *SandP1, num1, num2, MIUI, RHOI, RHOp and D* as Double Initialize Variable *MIUI* = 0.969214989500888 Initialize Variable *RHOI* = 57.7476207397836 Initialize Variable *RHOp* = 165.43409559 Initialize Variable *D* = 1.5 For *D* = 1.5:1.0:12.007 Calculate *SandP1 = (((num1) ^ 0.53) * (num2 ^ 0.17) * ((MIUl / RHOl) ^ (-0.09)) * (((RHOp - RHOl) / RHOl) ^ 0.55) * (D ^ 0.47)) ^ (1 / 1.53)* *Next* End
Vs	1: Particle Settling Velocity (Laminar) Determination	$u_t = \frac{g d_p^2 \left(\rho_p - \rho_l\right)}{18 \mu_l}$ Settling according to Stoke's Law for Laminar Settling	Program Start Declare Variable *PatTermSet, num, MIUI, RHOl, RHOp, Vel and g* as Double Initialize Variable *MIUI* = 0.969214989500888 Initialize Variable *RHOI* = 57.7476207397836 Initialize Variable *RHOp* = 165.43409559 Initialize Variable *g* = 32.174 Compute Re = (RHOl*Vel*D)/(MIUI) For Re<2000 Calculate *PatTermSet = (g * (num ^ 2) * (RHOp - RHOl)) / 18 * MIUl* Else Calculate *PatTermSet* = 1.73 * ((num * g) * ((RHOp - RHOl) / RHOl)) ^ (1 / 2) *Next* End
	2: Particle Terminal Settling Velocity (Turbulent) Determination	$u_t = 1.73 \sqrt{d_p g \left(\frac{\rho_p - \rho_l}{\rho_l}\right)}$ Settling according to Newton's Law for Turbulent Settling	Program Start Declare Variable *PatTermSet, num, MIUI, RHOl, RHOp, Vel and g* as Double Initialize Variable *MIUI* = 0.969214989500888 Initialize Variable *RHOI* = 57.7476207397836 Initialize Variable *RHOp* = 165.43409559 Initialize Variable *g* = 32.174 Compute Re = (RHOl*Vel*D)/(MIUI) For Re<2000 Calculate *PatTermSet = (g * (num ^ 2) * (RHOp - RHOl)) / 18 * MIUl* Else Calculate *PatTermSet* = 1.73 * ((num * g) * ((RHOp - RHOl) / RHOl)) ^ (1 / 2) *Next* End
	3: Kinematic Viscosity of Liquid Determination	$V_l = \frac{V_{SL}}{H_L}$ Known Relation	Program Start Declare Variable *KinVis, num, Hl* as Double Initialize Variable *Hl* = 0.507 Compute KinVis = num / Hl End

An Overview of VBA for Excel Codes Used to Determine Critical Sand up Velocities (Vc), Critical Erosional Velocities (Vs), Pressure Drop @ MTC and then its associated Critical Velocity Value (Vp), and the Critical Sand Concentrations (Cv).			
Value Being Determined	**Steps**	**Correlation**	**Sample VBA Code**
	4: Friction Velocity (Laminar) Determination	$u_0^* = \left[100 u_t \left(\frac{v_l}{d_p} \right)^{2.71} \right]^{0.269}$ Thomas (1961) Upper Model	Program Start Declare Variable *FricVel, num1, num2, num3 as* Double Compute FricVel = (100 * num1 * ((num2 / num3) ^ 2.71)) ^ 0.269 End
	5: Friction Velocity (Turbulent) Determination	$u_0^* = \left[0.204 u_t \left(\frac{v_l}{d_p} \right) \left(\frac{v_l}{D} \right)^{-0.6} \left(\frac{\rho_p - \rho_l}{\rho_l} \right)^{-0.23} \right]^{0.714}$ (Thomas (1961) Lower Model)	Program Start Declare Variable *FricVelT1, num1, num2, num3, RHOp, RHOl, D as* Double Initialize Variable MIUI = 0.969214989500888 Initialize Variable RHOI = 57.7476207397836 Initialize Variable RHOp = 165.43409559 Initialize Variable D = 12.007 Compute FricVelT1 = (0.204 * num1 * (num2 / num3) * ((num2 / D) ^ (-0.6)) * (((RHOp - RHOl) / RHOl) ^ (-0.23))) ^ 0.714 End
	6: Wall Shear Velocity Determination	$\tau_0 = \left(u_0^* \right)^2 * \rho_m$ (Modified Coulson et al (2010) Model)	Program Start Declare Variable *WalSVel, num and RHOs as* Double Initialize Variable RHOs = 32.1768837150703 Compute WalSVel = (num ^ 2) * RHOs End
	7: Dimensionless Liquid Flow Rate Determination	$\psi_L = \frac{\rho_l g d_p \left(\frac{\rho_p}{\rho_l} - 1 \right)}{\tau_0}$ (Gillies (1997) Correlation)	Program Start Declare Variable LiqRate, *num1, num2, RHOp, RHOl, g as* Double Initialize Variable RHOI = 57.7476207397836 Initialize Variable RHOp = 165.43409559 Initialize Variable g = 32.174 Compute LiqRate = (RHOl * g * num1 * ((RHOp / RHOl) - 1)) / num2 End
	8: Dimensionless Sand Transport Rate Determination	$\varphi_s = \left[\frac{4}{\psi_L} - 0.188 \right]^{1.5}$ (Gillies (1997) Model)	Program Start Declare Variable *SandRate and num as* Double Compute SandRate = ((4 / num) - 0.188) ^ 1.5 End

An Overview of VBA for Excel Codes Used to Determine Critical Sand up Velocities (Vc), Critical Erosional Velocities (Vs), Pressure Drop @ MTC and then its associated Critical Velocity Value (Vp), and the Critical Sand Concentrations (Cv).			
Value Being Determined	**Steps**	**Correlation**	**Sample VBA Code**
	9: Cross-Sectional Area of Pipe Determination	$A = \frac{\pi D_i^2}{4}$ (Known Relation)	Was Not Coded
	10: Critical Erosional Velocity Determination	$V_s = \frac{\varphi_s}{A}$ (Known Multiphase Relation)	Program Start Declare Variable *EroVel, num1 and num2 as* Double Compute EroVel = num1 / num2 End
Vp	11: Pressure Drop @ MTC Determination	$\left\|\frac{\Delta P}{\Delta x}\right\|_{MTC} = \frac{4\rho_l \left(u_0^*\right)^2}{g_c D}$ (King et al (2000) Model)	Program Start Declare Variable MTCp1, *num, D, RHOl, gc as* Double Initialize Variable RHOI = 57.7476207397836 Initialize Variable D = 1.5 Initialize Variable gc = 32.174 Compute MTCp1 = (4 * RHOl * (num ^ 2)) / (gc * D) End
	12: Critical Velocity at Pressure Drop Determination	$V_p = \left\|\frac{\Delta P}{\Delta x}\right\|_{MTC} \times \frac{\left(\frac{\mu_l}{\rho_l}\right) * 92903.039972}{MAOP}$ (Modelled from Known Multiphase Relations; MAOP = Maximum Allowable Operating Pressure 92903.039972 = Conversion Factor from Dynamic Viscosity (in cp) to Kinematic Viscosity (in ft^2/s))	Program Start Declare Variable PDFloVel, *num, MIUI, MAOP, RHOl as* Double Initialize Variable MIUI = 0.969214989500888 Initialize Variable RHOI = 57.7476207397836 Initialize Variable MAOP = 673 Compute PDFloVel = num * (((MIUl / RHOl) * 92903.039972) / MAOP) End
Cv	13: Critical Sand Concentration Determination	$C_v = \left(\frac{V_c}{\sqrt{gD}\,0.055 \left(\frac{d_p}{D}\right)^{-0.6} (s-1)^{0.07} \left(\frac{\rho_l u_t d_p}{\mu_l}\right)^{0.3}} \right)^{\frac{1}{0.27}}$ (Modified Kokpinar and Gogus (2000) Model) $s = \frac{\rho_p}{\rho_m}$ (Determining of s-value from Kokpinar and Gogus (2000) Model)	Program Start Declare Variable CSCSandP1, num1, num2, num3, MIUI, RHOI, RHOp, g and D as Double Initialize Variable MIUI = 0.969214989500888 Initialize Variable RHOI = 57.7476207397836 Initialize Variable RHOp = 165.43409559 Initialize Variable g = 32.2 Initialize Variable D = 1.5 Compute s = RHOp / RHOl CSCSandP1 = (num1 / ((g * D) ^ 0.5) * (0.055 * ((num2 / D) ^ (-0.6))) * ((s - 1) ^ 0.07) * (((RHOl * num3 * num2) / MIUl) ^ 0.5)) ^ (1 / 0.07) End

SAŽETAK

Kvantitativna procjena rizika utjecaja pijeska na višefazni protok u cjevovodu

Prisutnost čestica pijeska, koje zajedno s proizvodnim fluidom protječu cjevovodom, povećava vjerojatnost nastanaka kvara na cjevovodu. Rizik od kvara na cjevovodu uvelike ovisi (ili je dodatno potenciran ili je smanjen) o uvjetima protjecanja fluida u cjevovodu. U ovome su radu prikazani rezultati kvantitativne analize rizika utjecaja pijeska na cjevovode tijekom višefaznoga protjecanja u uvjetima nastanka kvara na cjevovodu: nakupljanja pijeska, erozije i pojave povećanoga gradijenta tlaka. U analizi su razmatrane tri komponente cjevovoda: cijev (nominalna veličina 1,5 in [3,8 cm]), ventil s povratnom zaklopkom (engl. *swing check valve*) (nominalna veličina 12,007 in [30,5 cm]) i LR koljeno od 90 stupnjeva (nominalna veličina 2,25 in [5,7 cm]). Korelacije, koje upućuju na kritične brzine i kritične koncentracije pijeska vrijednosti iznad ili ispod kojih se navedeni kvarovi cjevovoda javljaju, prikazane su u programu Visual Basic. Analiza je provedena na temperaturi od 204 °C i tlaku od 604 psi [4,2 × 106 Pa]. Distribucija vjerojatnosti, simulirajući realan scenarij, dobivena je korištenjem Monte Carlo simulacije. Utvrđena je vjerojatnost pojave kritičnih vrijednosti koncentracije pijeska, koje se nalaze izvan postavljenih statističkih granica, što upućuje na vjerojatnost pojave uzroka kvara koji se istražuje. Za sva tri uzroka kvara posljedice pojave (prikazane kapitalnim troškovima (CAPEX) sanacije nastalih kvarova) pomnožene su s vjerojatnošću kvara, čime je dobiven indeks rizika. Na temelju histogramskoga dijagrama prosječnoga indeksa rizika i analize, provedenim istraživanjem utvrđeno je da su komponente većega promjera sklone turbulenciji, što dovodi do većega rizika od erozije. Rizik od velikoga pada tlaka i nakupljanja pijeska bio je znatno manji od rizika od erozije (abrazije).

Ključne riječi:
prosječni promjer čestica, kritična koncentracija pijeska, nakupljanje pijeska, erozija, povećani gradijent tlaka, Monte Carlo simulacija

Author's contribution

U. I. Duru, designed the simulation work. While **C. Ndukwe** developed the VBA codes**, P.M Ikpeka** performed the Monte Carlo Simulation**. U. I. Duru** supervised the simulation work**. U.I. Duru and P.M. Ikpeka** analysed the results obtained and participated in writing the final draft. **A.O. Arinkoola** and **S.I. Onwukwe** cross-checked the codes and analysed the results obtained. The first draft was written by **U. I. Duru** and **P.M. Ikpeka.**